

Forecasting groundwater level fluctuations for rainfall-induced landslide

Yao-Ming Hong · Shiuan Wan

Received: 6 May 2009 / Accepted: 18 August 2010 / Published online: 5 September 2010
© Springer Science+Business Media B.V. 2010

Abstract Groundwater plays a critical and important role in many landslides. Heavy precipitation can raise the groundwater level within a hillslope and lead to instability. The purpose of this paper is to present a model by means of continuity equation to predict groundwater level fluctuations in hillslope in response to hourly precipitation rates. The linear reservoir method is employed to describe the travel time distribution of infiltration, and Darcy's law is then used to establish the groundwater flux rate of control volume. The governing equation shows that the changing rate of groundwater level fluctuation can be interpreted by two new defined variables (Sink Number and Rise Number) in this study. The application of the model is demonstrated using the rainfall-induced landslide at Lu-Shan, Nantou County, Taiwan. Data from one storm event are used to calibrate the model and estimate parameters by using the heuristic algorithm. Post-storm rainfall data from another storm event are employed to verify the calibrated parameters. The contribution of this study shows that a small Sink Number results in a fast recession and a large Rise Number yields a fast rise of groundwater level. This method may be practical to have better understanding on the rainfall-induced landslide.

Keywords Groundwater level fluctuation · Hillslope · Linear reservoir method · Rainfall-induced landslide

1 Introduction

Groundwater level modeling is important for environmental protection: maintaining the groundwater equilibrium system, controlling groundwater level fluctuation, and protecting against severe land subsidence. However, predicting the groundwater system is a complex

Y.-M. Hong (✉)

Department of Design for Sustainable Environment, MingDao University, 369 Wen-Hwa Rd., Peetow, Changhua 52345, Taiwan, R.O.C
e-mail: blueway@mdu.edu.tw

S. Wan

Department of Information Management, Ling Tung University, Taichung, Taiwan

nonlinear dynamic procedure. It involves nonstationary stochastic hydrological features by climate and land use characteristics.

Generally speaking, the groundwater level during heavy rainfall may induce the landslide occurrence. Considerable concerns have been arisen on the relationship between landslide, groundwater level, and rainfall intensity. For instance, Caris and Van Asch (1991) conducted the geophysical, geotechnical, and hydrological surveys in the French Alps on a small landslide in black marl material to assess the stability. Their analysis revealed that a groundwater level of 4 m below the ground surface is the critical threshold for reactivating the landslide. Van Asch et al. (1999) considered that deeper landslides (5–20 m depth) are the most cases triggered by positive pore pressures on the slip plane induced by a rising groundwater level. Mantovani et al. (2000) believed that landslide may be correlated with a sudden increase in the groundwater table, even though the extent of the rise was not among the highest recorded during the observation period. Schmidt and Dikau (2004) developed a process-based, spatio-temporal model for groundwater variations and slope stability using the GIS environment of the software PCRaster. Neaupane and Achet (2004) used antecedent rainfall, rainfall intensity, infiltration parameter, shear strength, groundwater, and steepness as the input parameters to build a back-propagation neural network for landslide monitoring. Trigo et al. (2005) proposed an important concept: translational slides, rotational slides, and complex and composite slope movements are triggered by groundwater level rising and the shear strength reduction. Ray and Jacobs (2007) also considered that most of the slope failures are caused by soil moisture or groundwater that increases pore water pressure and decreases shear strength. Gattinoni (2009) concluded that water is one of the main causes of landslide and the hazard assessment has to consider the groundwater setting and its effects on slope stability. To sum up, past studies focus on accurate slope-stability analysis of pre-existing landslides, and adjacent, potentially landslide-prone slopes requires a realistic estimation of maximum groundwater levels. Hence, a real-time precise prediction of groundwater level may render a great help on forecast the landslide occurrence.

A feasible solution in finding the relations between field measurement of groundwater level and precipitation has drawn a great attraction on scientists. Wu et al. (1996) found that in a soil profile with a shallow water table, the response of recharge to rainfall was very fast, and there was a close relation between them. Malet et al. (2005) thought that the combination of precipitation and rapid snowmelt induced the significant increase in the groundwater level, and the potential instability factor is the generation of high groundwater levels leading to excess pore water pressures. Szilagyi et al. (2005) analyzed total recharge to groundwater in Nebraska. They found that long-term mean recharge is greater than those of 140 mm per year. Schwartz and Schreiber (2009) found when the slope of cumulative precipitation is equal to or steeper (more positive) than that of potential evapotranspiration, potential recharge can occur. Abbasov and Mahmudov (2009) demonstrated that construction of dykes and levees does not actually prevent flooding, where hydrologic connections between groundwater and surface water are high, since infiltrated water from channel results in raising of groundwater, causing an effect of “underground flood.” Therefore, precipitation is one of the dominant factors contributing to groundwater level fluctuation.

A well-known groundwater flow model today, MODFLOW, adopted the finite difference approximation equation (Rushton and Redshaw 1979) to develop a physical-based governing equation, which can be used to simulate the flow of groundwater through aquifers (McDonald and Harbaugh 2003). This program provides a great contribution on groundwater level estimation. If the groundwater parameters of MODFLOW, such as

hydraulic conductivity, specific yield, specific storage, are accurately measured, the groundwater level can be forecasted rationally (Hunt et al. 2008). Also, MODFLOW can be successfully applied on the time scale of hours or even seconds. Unfortunately, difficulties are encountered if an iterative process of searching the values of related variables is required while using MODFLOW. That is, the processes of trial and error have to be done while applying MODFLOW if any of the related variables (hydraulic conductivity, specific yield, specific storage, etc.) is unknown.

In general, landslides usually take place after a few hours of the torrential precipitation. It is expected to develop an hourly prediction model of groundwater level with iterative (trial-and-error) process to calibrate the influence variables. In this study, a hydrological continuity equation is introduced to develop the forecasting model of groundwater level fluctuation on torrential precipitation. The travel time distribution of infiltration is estimated by the linear reservoir method. Darcy's law is used to describe the groundwater inflow/outflow process of control volume. Finally, we develop a governing equation, which is a combination of first-order linear differential equation and linear reservoir equation. A hybrid method, which uses the fourth-order Runge–Kutta method to solve the linear equation and adopts a heuristic algorithm based on root mean square error (RMSE) to obtain the representative values of groundwater parameters, is used to develop a computer program. In our study, two composite variables are generated: (1) Sink Number represents the recession characteristics of groundwater level. (2) Rise number represents the rising characteristics of groundwater level. Applying these two variables in our model, theoretically, the results of groundwater level fluctuation can be calibrated rationally. To test this model, this study calibrates the groundwater parameters by the precipitation and groundwater level data of a given storm. The calibrated model considering an independent post-calibration data set is also verified.

2 The forecasting method on the development of groundwater level

2.1 Governing equation of groundwater level fluctuation

Figure 1a describes the water travel process from precipitation to stream. Due to the gravity effect, precipitation falls into the ground and then infiltrates into the soil. After a period of time, water reaches the aquifer region and flows into the downstream following the impervious layer. The hydrological continuity equation (Chow et al. 1988) is used to describe the movement of water in the soil as follows:

$$\frac{dS}{dt} = I - O \quad (1)$$

where S is the storage volume of control volume; I is the inflow rate, including infiltration recharge rate and groundwater inflow rate; O is the groundwater outflow rate.

S can be described as the groundwater storage with an aquifer region of unit area L (Rasmussen and Andreasen 1959)

$$S = phL \quad (2a)$$

where p is the fillable porosity as the volume of water per unit area L required for a unit rise of the water table (Sophocleous 1991; Maréchal et al. 2006; Park and Parker 2008). The differential analysis of S to time is

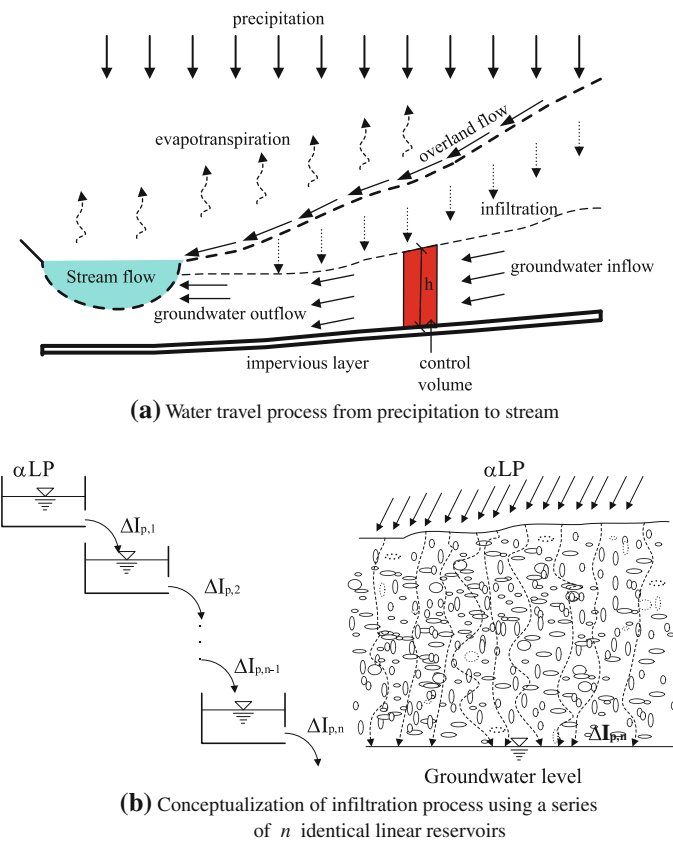


Fig. 1 Conceptual sketch of groundwater travel process

$$\frac{dS}{dt} = pL \frac{dh}{dt} \quad (2b)$$

2.2 Infiltration recharge rate

From Fig. 1a, the water inflow rate can be displayed as

$$I = I_p + I_g \quad (3a)$$

where the groundwater inflow rate I_g will be discussed with groundwater outflow rate; I_p is the infiltration recharge rate, which is the difference between precipitation rate P_r and the sum of evapotranspiration rate E_r , overland flow O_r , and soil keeping water rate S_r as follows

$$I_p = [P_r - (E_r + O_r + S_r)]L \quad (3b)$$

There have been numerous studies in the literature dealing with the relationship between infiltration recharge rate and precipitation. Wu et al. (1996) obtained a regression equation for the relationship between precipitation and recharge by infiltration as follows

$$I_{p,e} = 0.87(P_{r,e} - 5.25) \quad (3c)$$

where $I_{p,e}$ is the recharge by infiltration of an individual precipitation event (mm), $P_{r,e}$ is the precipitation (mm), and the constant 5.25 mm is the threshold value of individual precipitation events, below which no recharge reaches the groundwater.

Park and Parker (2008) assumed daily recharge rate $I_{p,d}$ can be approximated as a fixed fraction of daily precipitation $P_{r,d}$ as

$$I_{p,d} = \alpha P_{r,d} L \quad (3d)$$

where α represents the infiltration ratio of precipitation. Above-mentioned I_p is a function of P_r , where Eq. (3c) is suitable to an individual precipitation event and Eq. (3d) is applied to a daily precipitation.

Li et al. (2005) conducted a field experiment in Hong Kong and observed where it has 3 day's lag between the highest precipitation and highest groundwater level. This is possibly due to the great infiltration of soil pore water flow after a heavy rainfall. USGS (U. S. Geological Survey 2009) observed a landslide in Honolulu, Hawaii. They discovered that rainfall can trigger surprisingly rapid rises in shallow groundwater. Above field experiments illustrated that a time lag exists between precipitation and groundwater level fluctuation.

On the other hand, Gelhar and Wilson (1974) showed that the water balance for an unconfined aquifer can be simplified to a linear relationship between the average water level and the rate of discharge, in case of the water level is quite small to be compared with the total thickness of an aquifer. Pulido-Velazquez et al. (2005) analyzed the structure of a stream–aquifer flow exchange solution, derived from the linear groundwater flow equation, to reveal that stream–aquifer interaction can be conceptualized as the drainage of an infinite number of independent linear reservoirs.

Generally speaking, the aforementioned methods assumed that linear reservoir method considered the aquifer as a reservoir. However, the linear reservoir model may be used to simulate the travel time distribution of infiltration. The time lag and infiltration rate between unit precipitation and infiltration recharge may be represented by a series of n identical linear reservoirs, each having the same storage constant β . This study assumes that the infiltration region is a series of reservoir (Fig. 1b) in which the discharge of first reservoir $\Delta I_{p,1}(t)$ is a linear function of the precipitation storage (storage of first reservoir) $\alpha LP(t)$:

$$\Delta I_{p,1}(t) = \frac{\alpha LP(t)}{\beta} \quad (3e)$$

Using the hydrological continuity equation, the infiltration pulse recharge rate (the discharge of nth linear reservoir) can be derived as follows:

$$\Delta I_{p,n}(t) = \frac{\alpha LP(t)}{\beta(n-1)!} \left(\frac{t}{\beta} \right)^{n-1} e^{-\frac{t}{\beta}} = \alpha LP(t) H(t) \quad (3f)$$

where $H(t) = \frac{1}{\beta(n-1)!} \left(\frac{t}{\beta} \right)^{n-1} e^{-\frac{t}{\beta}}$ is a unit pulse of infiltration recharge rate. In addition, the peak pulse of infiltration recharge rate H_p and the peak time t_p can be obtained by differencing $H(t)$ as follows

$$t_p = \beta(n-1) \quad (3g)$$

$$H_p = \frac{1}{\beta(n-1)!} (n-1)^{n-1} e^{-(n-1)} \quad (3h)$$

where a large t_p represents a long time lag between unit precipitation and maximum infiltration rate; a small H_p denotes a small peak pulse of infiltration recharge rate. Equations (3g) and (3h) illustrate that a large β and a large n result in a long time lag and a small peak pulse of infiltration recharge rate.

Let the time domain can be separated into discrete intervals of duration Δt . Assuming P_m is the depth of precipitation during the time interval between $(m-1)\Delta t$ and $m\Delta t$. The infiltration recharge rate in the N th time interval ($t = N\Delta t$) is

$$\begin{aligned} I_{p,N}(t) &= \alpha L(P_1 H(N\Delta t) + P_2 H[(N-1)\Delta t] + \cdots + P_m H[(N-m+1)\Delta t] + \cdots + P_N H[\Delta t]) \\ &= \alpha L \sum_{m=1}^N P_m H[(N-m+1)\Delta t] \end{aligned} \quad (3i)$$

where N is the influence range of infiltration pulse recharge rate depending on the parameters n and β .

2.3 Horizontal flow rate of groundwater

Figure 2a illustrates the relationship between horizontal groundwater inflow rate I_g and horizontal groundwater outflow rate O_g .

By Darcy's law, the groundwater inflow rate is

$$I_g = k \frac{\Delta h_2}{\Delta x} h_2 \quad (4a)$$

where k is the hydraulic conductivity; $\frac{\Delta h_2}{\Delta x}$ is the inflow hydraulic gradient; h_2 is the inflow cross-section area of unit width. The groundwater outflow rate is

$$O_g = k \frac{\Delta h_1}{\Delta x} h_1 \quad (4b)$$

where $\frac{\Delta h_1}{\Delta x}$ is the outflow hydraulic gradient; h_1 is the outflow cross-section area of unit width. Assuming the local groundwater gradient in control volume is the same as the regional gradient, i.e., $\frac{\Delta h_2}{\Delta x} = \frac{\Delta h_1}{\Delta x} = \frac{\Delta h}{\Delta x}$, then the difference between I_g and O_g is

$$I_g - O_g = k \left(h_2 \frac{\Delta h_2}{\Delta x} - h_1 \frac{\Delta h_1}{\Delta x} \right) = -kL \frac{\Delta h}{\Delta x} (h_1 - h_2) = -kLi \frac{\Delta h}{\Delta x} \quad (4c)$$

where $i = \frac{h_1 - h_2}{L}$, is the mean hydraulic gradient of control volume. Park and Parker (2008) assumed net storage change due to groundwater flow to be proportional to groundwater storage such that

$$I_g - O_g = KS = KpLh \quad (4d)$$

where $K = \frac{-ki\Delta h}{ph \Delta x}$ is a transportable parameter of groundwater. They assumed $L \cong \Delta x$ and $(h_1 - h_2) \cong \Delta h$, then $\frac{\Delta h}{\Delta x} \cong i$ and $K = -\frac{ki^2}{ph}$. Because of i^2 , k , p , and h are positive number, K is always negative. In some cases, h_1 is not always greater than h_2 . This is based on the

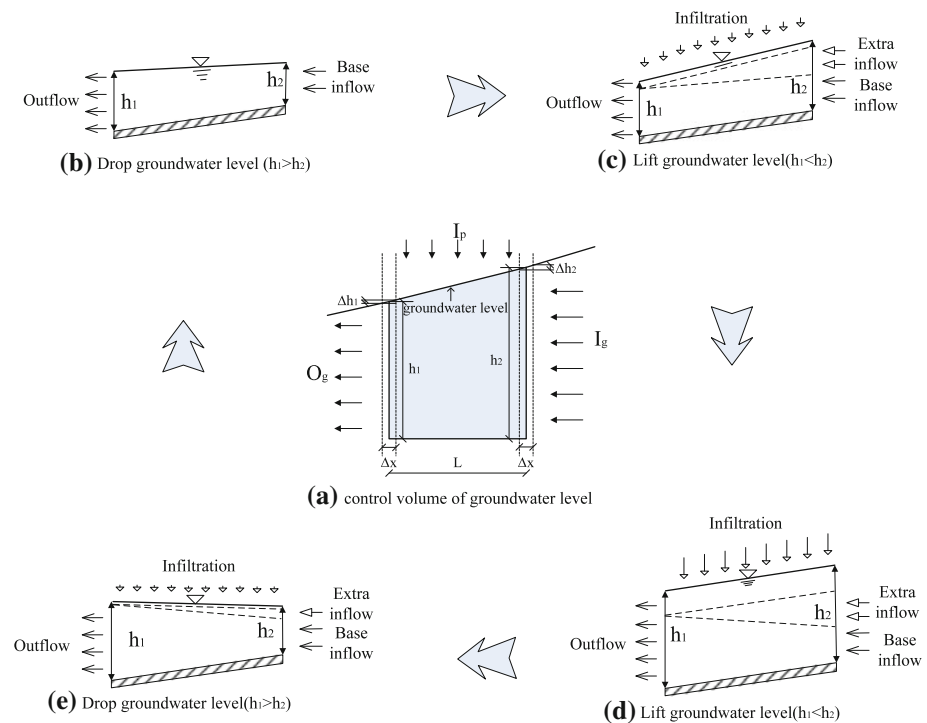


Fig. 2 Groundwater level fluctuation of control volume during torrential precipitation

groundwater level fluctuation circle during storm different periods. We divide the groundwater level fluctuation loop into four stages as follows:

(1) No infiltration stage (Fig. 2b)

When no precipitation occurs, groundwater outflow rate is bigger than groundwater inflow rate, which is defined as base inflow, so as to reduce the groundwater level. Owing to $(h_1 - h_2) > 0$, Eq. (4d) can be used in this stage.

(2) Initial stage of infiltration (Fig. 2c)

In the early stage of infiltration, a little infiltration and extra groundwater inflow from upstream raise the groundwater level. In this stage, $(h_1 - h_2) < 0$. Hence, Eq. (4d) only satisfies the relationship between base inflow and outflow. Extra groundwater inflow should be estimated appropriately by other method.

(3) Stage of large infiltration and great extra groundwater inflow (Fig. 2d)

In this stage, increasing infiltration and extra groundwater inflow quickly lift the groundwater level. Extra groundwater inflow also should be estimated appropriately.

(4) Stage of small infiltration and little extra groundwater inflow (Fig. 2e)

When precipitation has stopped for a period of time, infiltration rate and extra inflow become small gradually. Finally, infiltration and extra inflow are very close to zero, and the groundwater level returns to no infiltration stage.

In general, the extra groundwater inflow comes from the infiltration recharge of upstream watershed. Hence, this study uses the linear reservoir method to estimate the extra groundwater inflow as:

$$I_g - O_g = KpLh + A\alpha L \sum_{m=1}^N P_m H[(N-m+1)\Delta t] \quad (4e)$$

where A is a constant depending on the groundwater watershed area.

3 Numerical method development

3.1 Groundwater level fluctuation equation

Substituting Eqs. (2b), (3i), and (4e) into Eq. (1) and then dividing Eq. (1) by pL yield

$$\frac{\Delta h}{\Delta t} = Kh + I \sum_{m=1}^N P_m H[(N-m+1)\Delta t] \quad (5a)$$

where $I = \frac{a}{p}(A+1)$ is always bigger than zero, and defined as the Rise Number. The term of $I \sum_{m=1}^N P_m H[(N-m+1)\Delta t]$ is the infiltration recharge and extra groundwater inflow. K is defined as the Sink Number that is always smaller than zero. Kh is the head loss of groundwater level.

According to Eq. (5a), the influence factors of groundwater level fluctuation can be separated into two parts:

- (1) The head loss due to flow flux of groundwater would reduce the groundwater level.
- (2) The infiltration recharge and extra inflow would raise the groundwater level.

On the other hand, Eq. (5a) is a combination of first-order linear differential equation and a linear reservoir equation, which can be solved by the numerical method such as the classical fourth-order Runge–Kutta method (Chapra and Canale 1988; Anderson and Woessner 1992; Hong 2008). First, Eq. (5a) can be conducted as

$$\frac{\Delta h}{\Delta t} = f(t, h) \quad (5b)$$

Defining $t_i = \Delta t \times i$ and the corresponding groundwater level is h_i , then

$$C_1 = f(t_i, h_i) = Kh_i + I \sum_{m=1}^N P_m H[(N-m+1)\Delta t] \quad (5c)$$

$$\begin{aligned} C_2 &= f\left(t_i + \frac{\Delta t}{2}, h_i + \frac{\Delta t}{2} C_1\right) \\ &= K\left(h_i + \frac{\Delta t}{2} C_1\right) + \frac{1}{2} \left(I \sum_{m=1}^N P_m H[(N-m+1)\Delta t] + I \sum_{m=2}^{N+1} P_m H[(N-m+1)\Delta t] \right) \end{aligned} \quad (5d)$$

$$\begin{aligned}
C_3 &= f\left(t_i + \frac{\Delta t}{2}, h_i + \frac{\Delta t}{2}C_2\right) \\
&= K\left(h_i + \frac{\Delta t}{2}C_2\right) + \frac{1}{2}\left(I \sum_{m=1}^N P_m H[(N-m+1)\Delta t] + I \sum_{m=2}^{N+1} P_m H[(N-m+1)\Delta t]\right)
\end{aligned} \tag{5e}$$

$$C_4 = f(t_i + \Delta t, h_i + \Delta t C_3) = K(h_i + \Delta t C_3) + I \sum_{m=2}^{N+1} P_m H[(N-m+1)\Delta t] \tag{5f}$$

where P_{N+1} is the precipitation occurred in $N\Delta t$ time. To take a closer observation, the precipitation depth at the time step $t_i + \frac{\Delta t}{2}$ is unknown; hence, the term of $\frac{1}{2}\left(I \sum_{m=1}^N P_m H[(N-m+1)\Delta t] + I \sum_{m=2}^{N+1} P_m H[(N-m+1)\Delta t]\right)$ is used as the infiltration rate and extra inflow occurred at the time of $t_i + \frac{\Delta t}{2}$. According to the fourth-order Runge–Kutta method, the groundwater level h_{i+1} at the time step t_{i+1} can be resolved by

$$h_{i+1} = h_i + \frac{\Delta t}{6}(C_1 + 2C_2 + 2C_3 + C_4) \tag{5g}$$

Equation (5g) illustrates that the groundwater level at time t_{i+1} can be computed by the measured groundwater level at time step t_i with a series of precipitation records.

3.2 Interval estimation of groundwater parameters from past literatures

From Eqs. (3i) and (5a), if n , β , N , I and K are determined, respectively, the groundwater level at time h_{t+1} can be determined by known h_t and a series of precipitation. Therefore, the proper ranges on the selection of K , I , n , N , and β could improve the prediction accuracy of groundwater level. The range in the estimation of groundwater parameters are described as follows:

(1) Travel time distribution of infiltration recharge rate (n , β , N)

Van Asch et al. (1999) chose one week as observed duration to make good correlations between precipitation and the frequency of landslides. Some field monitoring data obtained by Lee et al. (2006) showed that the time lag for peak precipitation and peak groundwater level may bring into half day to twenty days behind. They also observed that the majority of rapid responses are during the winter/spring recharge period. In the mean time, the unsaturated zone is thinnest and the unsaturated zone moisture content is highest. That is, the time lag is a function of the thickness of unsaturated zone, seasons, and precipitation intensity. Park and Parker (2008) used one day's precipitation to calculate the infiltration in next day. According to Eqs. (3g) and (3h), n and β control the travel time distribution of infiltration recharge rate. Due to the application domain of this study is constrained by means of the hillslope and torrential precipitation, this study selects a short time lag with $1 \leq \beta \leq 4$ and $2 \leq n \leq 5$. If $\Delta t = 2$ h, the shortest time lag t_p is 2 h, and the longest is 32 h by Eq. (3g). In addition, this study uses $N = 40$.

(2) Infiltration ratio of precipitation (α)

In the second part of the study, infiltration ratio of precipitation is studied. Numerous methods on the estimate of infiltration ratio of precipitation are done. For example, Bhark and Small (2003) observed precipitation and infiltration for the four rainfall events to

obtain the infiltration ratio range of 60 to 85%. Li et al. (2005) conducted a full-scale field experiment in an instrumented saprolite slope and found that infiltration was around 70% of the total rainfall. According to above studies, we adopt the infiltration ratio range (α) of 0.5 to 1.

(3) Fillable porosity (p)

The third part of this study, the fillable porosity, has to be discussed. Sophocleous (1991) measured the mean effective storativity of field data collection for 5 different sites. The range of effective storativity is the range of 0.046–0.058. State of florida department of transportation (2004) adopted (p) in the range of 0.1–0.3. For conservative propose, this study chooses the fillable porosity (p) of 0.05–0.5.

(4) Rise Number (I)

In this study, an artificial variable is generated to represent the rising level of groundwater level under precipitation—Rise Number. Using the limit of (α) and (p), the ratio of $\frac{\alpha}{p}$ is in the range of 1–20. Park and Parker (2008) used $\frac{\alpha}{p} = 8$, which was determined by nonlinear regression to minimize the root mean square (RMS) deviation between observed and predicted water levels for the calibration period. In addition, this study assumes A in the range of 1 to 5, to represent the ratio between extra groundwater inflow and infiltration directly from vertical precipitation. Therefore, we obtain the Rise Number (I) in the range of 2–48.

(5) Sink Number (K)

In this study, another artificial variable is generated to represent the sinking level of groundwater level—Sink Number. Park and Parker (2008) adopted the Sink Number $K = -0.15/\text{day}$ in the Hongcheon area of South Korea. If the unit time is 2 h, then $K = -0.0125/(2 \text{ h})$. This study assumes K in the range of -0.02225 and -0.0005 .

3.3 Computer program development and use

Figure 3 depicts the steps of groundwater level forecasting method, which can be separated into four parts as follows:

(1) Data collection

In this stage, the necessary data should be collected below:

- We suggest that the sampling interval is to use one or 2 h to monitor the precipitation depth and the groundwater level.
- Geographic information such as topography, location and depth of well, and location of rainfall station renders helpful information to determine the groundwater datum and select suitable well, which has obvious response when precipitation occurs.

(2) Raw data reduction

The raw data in this study contain records of several years. The storm with maximum cumulative precipitation volume may be the optimal candidate of training sample. All the groundwater level records of all wells with respect to each well are carefully checked to select the appropriate wells to present the collection between groundwater level and precipitation. Finally, we will obtain a series of training samples, which may have the records of one storm including precipitation depth, groundwater levels of several wells.

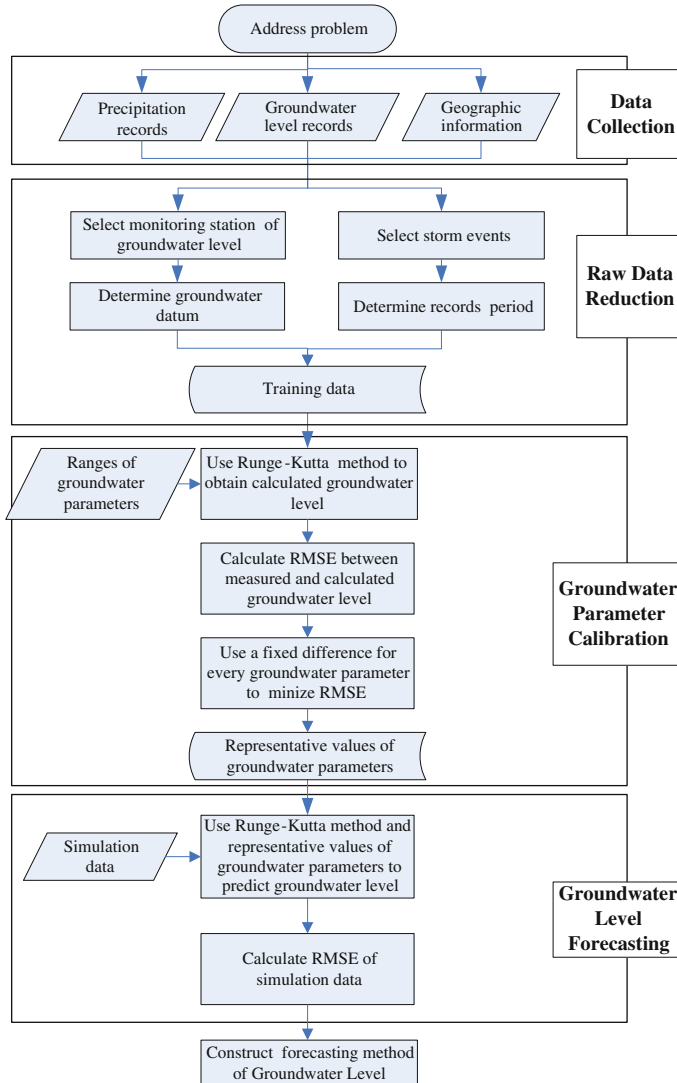


Fig. 3 Use step for groundwater level forecasting

(3) Groundwater parameters calibration

Calibration of a flow model refers to a model capable of producing field-measured heads and flows (Anderson and Woessner 1992). This study develops a computer program by visual C++ 6.0 to execute the calibration and simulation works. First, the fourth-order Runge-Kutta method is used to calculate h_{t+1}^p , and then, RMSE E_p are used to quantify the average error in the calibration as follows (Anderson and Woessner 1992):

$$E_p = \sqrt{\frac{\sum_{i=1}^n (h_{t+1}^p - h_{t+1}^m)^2}{n}} \quad (6)$$

Table 1 Groundwater parameters selection of model

Parameter	Minimum value	Increment for every loop	Counter numbers for every parameter	Maximum value
K	-0.02225	0.00075	30	-0.0005
β	1	1	4	4
n	2	1	4	5
I	2	2	25	48

where E_p is the average of the squared differences in measured and predicted groundwater level; n is the record number in a storm; h_{i+1}^p is the predicted groundwater level at time $i + 1$; h_{i+1}^m is the measured groundwater level at time $i + 1$.

The trial-and-error calibration is used to find the representative values of groundwater parameters with minimal RMSE. Specifically, the subroutine of this program is designed to control the groundwater parameters with fixed increment in given range, and the RMSE is computed for every iteration step. Table 1 displays the range of groundwater parameters and the increment interval for each iteration step.

(4) Groundwater level forecasting

The representative values of groundwater parameters are plugged into our developed program. The real time of next steps of groundwater level can be predicted based on the current step of precipitation depth and groundwater level. RMSE will also be calculated for the agreements of verification.

4 Field application and discussion

4.1 Field description and groundwater parameters determination

In Taiwan, summer heavy precipitation usually induces hazards such as landslide, mudslide, debris flow or flood, which may result in enormous losses. An attempt on further study, the landslide area at Lu-Shan, Nantou county, Taiwan, is chosen as the field test area for the groundwater level fluctuation on torrential precipitation. This landslide area is 0.54 km² with an average slope of 54°. In the past, typhoon often brings heavy precipitation to trigger landslides in this area; the Soil and Water Conservation Bureau (SWCB) mounted ten wells to monitor the groundwater level in 2005. In addition, there were 145 monitoring points and four reference points controlled by Global Position System (GPS). They were distributed in the field for measuring the surface movement. Another ten inclinometers were set up to observe the underground movement. Figure 4 is the topography of landslide area, which shows that the wells B03 and B06 are located in the lower elevation of this zone, which may collect more water than those of the other wells.

Figure 5a is the daily precipitation depth in the period of 2005/7/14 to 2005/10/9. Two typhoon named Haitang (7/17/2005–7/22/2005) and Matsa (8/4/2005–8/9/2005) brought a large amount of rainfall, which lead to the violent fluctuation of groundwater level (Fig. 5b and c) and the landslide movement in the range of 5 cm to 15 cm. Figure 5b and c show that the wells B03 and B06 have obvious change when torrential precipitation occurs. Therefore, this study chooses the data from these two wells to test the model.

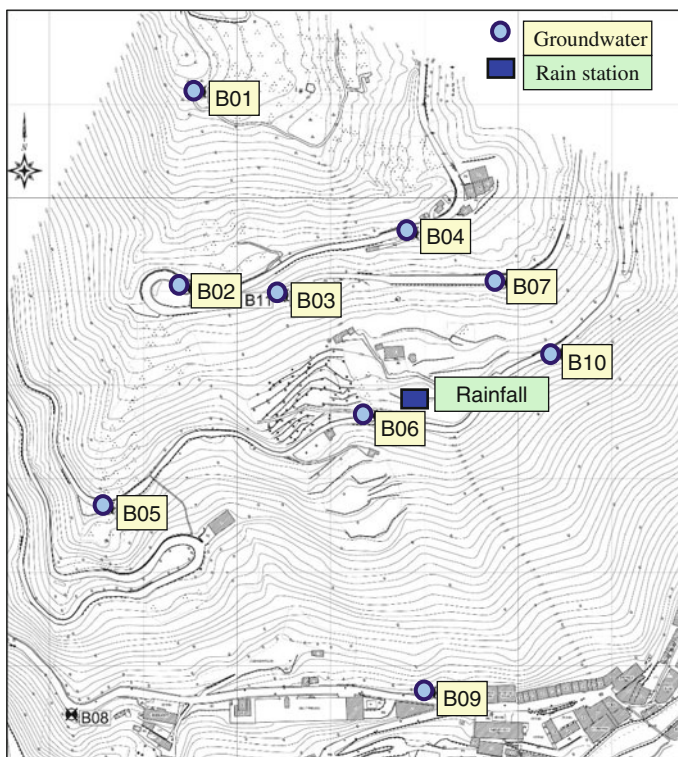


Fig. 4 Topographic map of landslide at Lu-Shan, Nantou county, Taiwan

This study obtains the representative values of groundwater parameters by using the Haitang typhoon, where the accumulative precipitation depth reached to 486.5 mm. According to the records of groundwater level, this study chooses a suitable elevation as the virtual datum. The average depth is between 7.75 m (B03) and 8.05 m (B06) above virtual datum; thus, it is expected to form the similar groundwater depth condition for all of the wells. The maximum difference of groundwater level is 10.68 m (B03) and 10.79 m (B06).

It is expected to use developed program to attain the representative values of groundwater parameters and RMSE. Table 2 displays a big Rise Number I and a short peak time $t_p (= \beta(n - 1))$ for both wells, which implies that the storm can quickly raise the groundwater level in this landslide. On the other hand, Table 2 also presents a small Sink Number, which may induce a slow recession rate of groundwater level.

4.2 Forecasting of groundwater level during torrential precipitation

This study uses the representative values of groundwater parameters to forecast the groundwater levels of Masta typhoon, where the accumulative precipitation depth reached to 562.5 mm (Fig. 6a). Figure 6b and c display the comparison between forecasting and measured groundwater level, where the RMSE is 18.68 cm (B03) and 18.04 cm (B06). They are slightly greater than the RMSE during the calibration process. The groundwater level graphs of two wells have the phenomena of quick rise and slow sink, which produce a large Rise Number and small Sink Number obtained in the calibration procedure.

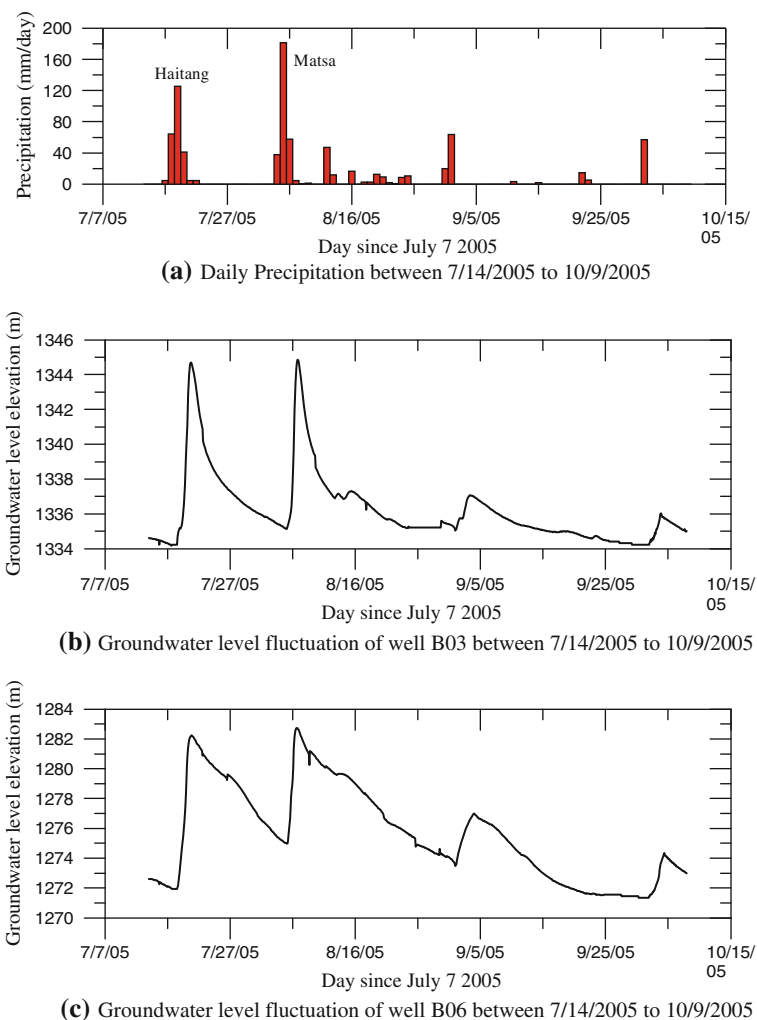


Fig. 5 Precipitation and groundwater level between 7/14/2005 to 10/9/2005

Table 2 Groundwater parameters and RMSE of wells

Well no.	K	β	n	I	RMSE (cm)			Predicted efficiency E_i (%)
					Training	Simulated E_p	Measured E_o	
B03	-0.00601	2	3	34	13.82	18.68	31.13	40.00
B06	-0.00451	1	2	31	9.53	18.04	26.53	32.00

A fundamental question arises: How efficiency is this method applicable to the forecasting of groundwater level? Differences in time steps of groundwater levels are generated as a series of E_o . Written it mathematically,

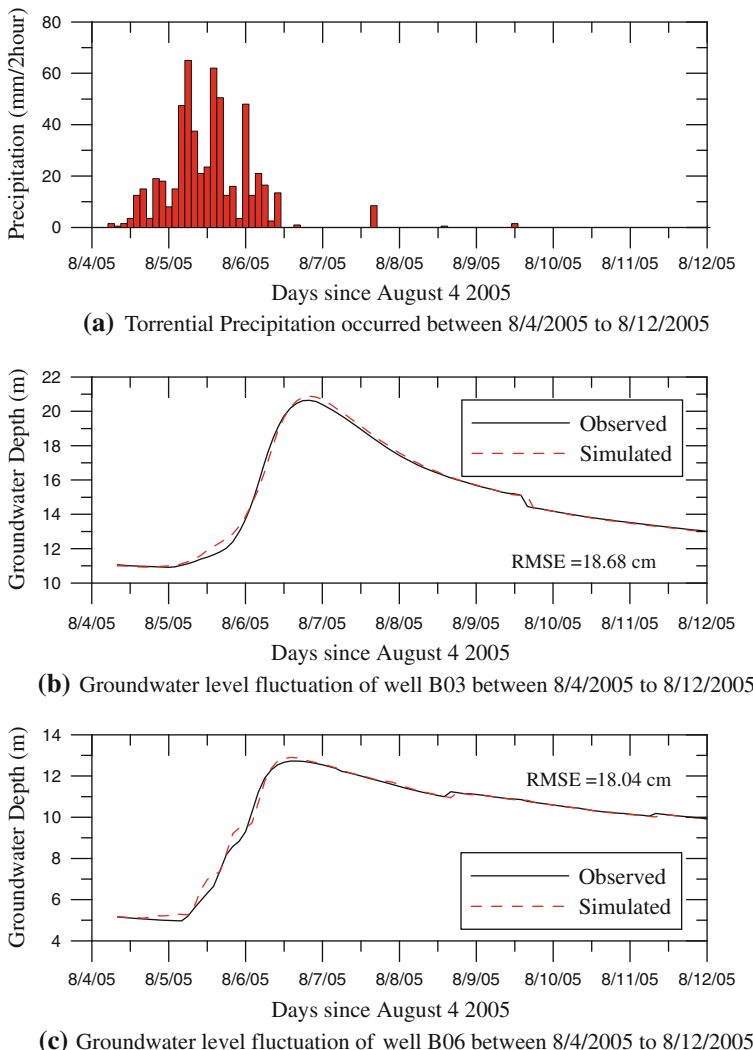


Fig. 6 Precipitation and groundwater level between 8/4/2005 to 8/12/2005

$$E_o = \sqrt{\frac{\sum_{i=1}^n (h_i^m - h_{i+1}^m)^2}{n}} \quad (7a)$$

where h_i^m is the measured groundwater level at i time, which is used as the predicted value at $i + 1$ time. E_o is the measured RMSE. A low E_o presents a mild groundwater fluctuation.

In addition, we define “predicted efficiency” E_i of predicted E_p and measured E_o as follows:

$$E_i = \frac{|E_p - E_o|}{E_o} \times 100\% \quad (7b)$$

A high and positive E_i indicates that the groundwater level prediction method is accurate and useful. Table 2 illustrates that the predicted efficiency is 40% (B03) and 32% (B06), respectively. In other words, this study can improve the predict accuracy of groundwater level between 32 and 40%.

4.3 The characteristics and influence of groundwater parameters

This study concludes the influence factors of groundwater level including Rise Number, Sink Number, and travel time distribution of infiltration recharge rate. This section discusses the possible change and comparison as follows:

(1) Rise Number

The process of groundwater level fluctuation can be divided into four stages. As aforementioned, Rise Number is introduced to interpret the characteristics of infiltration ratio, fillable porosity, and extra inflow rate of groundwater by upstream infiltration. A large Rise Number should yield a fast rise of groundwater level after precipitation beginning. The Well B03 and B06 have large Rise Numbers; it can be inferred that the rising slope of groundwater level should be steep. This can also be seen in Fig. 5b and c. The Rise Numbers shown in Table 2 are bigger than the maximum value of $\frac{\alpha}{\beta}$. Therefore, groundwater levels in the well B03 and B06 may be sensitive to upstream groundwater during the torrential precipitation period. In other words, if we can decrease the Rise Number such as exhausting upstream groundwater (reducing the value of A) or discharging the surface flow (reducing α), we can reduce the groundwater level to avoid the landslide occurrence.

(2) Sink Number

According to the definition of Sink Number, a small Sink Number should induce a fast recession rate of groundwater level after precipitation stop. If the real Sink Number is small and the selected Sink Number is big, then the sink slope of predicted groundwater level will be milder than that of real groundwater level. We found that the Sink Number of well B03 (-0.00601) is smaller than that of well B06 (-0.00451) and the recession rate of well B03 should be faster than that of well B06. This phenomenon can also be confirmed with Fig. 5b and c.

In general, the elevation of impervious layer is unknown. It can be presumed an elevation as the datum of impervious layer. If we change the datum, the groundwater parameters may be changed simultaneously. Two different cases are shown to test the sensitivity of groundwater parameters: (1) case1: reduces 50 m through yielded $K = -0.00151$ and (2) case2: decreases 100 m through yielded $K = -0.0008$ of groundwater datum, respectively. Obviously, β , n , I , and RMSE do not change. Therefore, it can be inferred that the Sink Number may be sensitive to the thickness of groundwater depth.

(3) Travel time distribution of infiltration recharge rate

The combination of β and n represents the time lag between unit precipitation and maximum infiltration ratio. Using Eq. (3g), we obtain the time lag t_p between unit precipitation and peak infiltration: well B03 has 4 h and well B06 has 1 h. A small t_p represents a short time lag between unit precipitation and peak recharge induced by unit precipitation. Table 3 shows the center of precipitation hyetograph, time of peak groundwater level, and the measured/calculated time lag T_p . A small T_p presents a short

Table 3 Time lag between the center of precipitation hyetograph and peak groundwater level

Well no.	Data source	Center of precipitation hyetograph	Time of peak groundwater level	Measured Time lag T_p (hour)	Peak time t_p (hour)	Lag constant C
3	Training	2005/7/19 12:00	2005/7/20 18:00	30	4	7.5
	Simulated	2005/8/5 13:00	2005/8/6 20:00	31	4	7.75
6	Training	2005/7/19 12:00	2005/7/20 20:00	32	1	32
	Simulated	2005/8/5 13:00	2005/8/6 14:00	25	1	25

time lag between peak precipitation and peak groundwater level. Assuming $T_p = C \times t_p$, in which C is a lag constant. These examples show that the same wells have same order of degree of time lag between unit infiltration and measured peak groundwater level, but in different wells, they behave totally different. This could be the discrepancy of environmental conditions (geology factors and precipitation hyetograph) to produce different outcomes.

5 Conclusion

In this paper, a numerical method for estimating groundwater level fluctuation in response to precipitation was developed based on the hydrological continuity equation in unconfined aquifers. A rainfall-induced landslide, located at Lu-Shan, Nantou county, Taiwan, is chosen as the field test area. Four of these findings are:

1. This study summarized the influence factors of groundwater level including: (a) A high infiltration ratio, a low fillable porosity, and extra inflow rate of groundwater due to upstream infiltration can raise groundwater level. A Rise Number is introduced to represent above three factors; (b) The sink rate of groundwater level is the function of hydraulic conductivity, fillable porosity, and head loss slope. A Sink Number is launched to employ these three factors; and (c) Travel time distribution of infiltration recharge rate can be represented by the linear reservoir method.
2. The comparison on RMSE between predicted and measured groundwater levels is at satisfactory agreement, which indicates that the method can be successfully calibrated with limited numbers of data and it can be practically improved the investigation into groundwater level.
3. A large Rise Number yields a fast rise rate of groundwater level from the start of the precipitation. The Rise Numbers of B03 and B06 are bigger than those of the maximum values of $\frac{z}{p}$. This shows that well B03 and B06 may be sensitive to upstream groundwater during the torrential precipitation period. On the other hand, a small Sink Number induces a fast recession rate of groundwater level after the stop of the precipitation. If the storm records including precipitation and groundwater level can be obtained, we can achieve the rise/sink characteristics of groundwater level mathematically.
4. It is clear from these examples that Sink Number is depending on the impervious datum. A thick soil depth will induce a large Sink Number. We can use any datum elevation as virtual datum to ignore the prediction error. We also found that a small Sink Number in the given area will induce a fast recession rate.

References

- Abbasov RK, Mahmudov RN (2009) Analysis of non-climatic origins of floods in the downstream part of the Kura River, Azerbaijan. *Nat Hazards* 50:235–248
- Anderson MP, Woessner WW (1992) Applied groundwater modeling, simulation of flow and advective transport. Academic Press, San Diego
- Barkay EW, Small EE (2003) Association between plant canopies and the spatial patterns of infiltration in shrubland and grassland of the Chihuahuan Desert, New Mexico. *Ecosystems* 6:185–196
- Caris JPT, van Asch TWJ (1991) Geophysical, geotechnical and hydrological investigations of a small landslide in the French Alps. *Eng Geol* 31(3–4):249–276
- Chapra SC, Canale RP (1988) Numerical methods for engineers, 2nd edn. McGraw-Hill, New York, pp 453–455
- Chow VT, Maidment DR, Mays LW (1988) Applied hydrology. McGraw-Hill, Singapore, pp 242–264
- Gattinoni P (2009) Parametrical landslide modeling for the hydrogeological susceptibility assessment: from the Crati Valley to the Cavallerizzo landslide (Southern Italy). *Nat Hazards* 50:161–178
- Velgar LW, Wilson JL (1974) Ground-water quality modeling. *Groundwater* 12:399–408
- Hong YM (2008) Graphical estimation of detention pond volume for rainfall of short duration. *J Hydro Environ Res* 2:109–117
- Hunt RJ, Prudic DE, Walker JF, Anderson MP (2008) Importance of unsaturated zone flow for simulating recharge in a humid climate. *Ground Water* 46(4):551–560
- Lee LJE, Lawrence DSL, Price M (2006) Analysis of water-level response to rainfall and implications for recharge pathways in the Chalk aquifer, SE England. *J Hydrol* 330:604–620
- Li AG, Yue ZQ, Tham LG, Lee CF (2005) Field-monitored variations of soil moisture and matric suction in a saprolite slope. *Can Geotech J* 42:13–26
- Malet JP, Laigle D, Remaître A, Maquaire O (2005) Triggering conditions and mobility of debris flows associated to complex earthflows. *Geomorphology* 66:215–235
- Mantovani F, Pasuto A, Silvano S, Zannoni A (2000) Collecting data to define future hazard scenarios of the Tessina landslide. *Int J Appl Earth Observation Geoinformation* 2(1):33–40
- Maréchal JC, Dewandel B, Ahmed S, Galeazzi L, Zaidi FK (2006) Combined estimation of specific yield and natural recharge in a semi-arid groundwater basin with irrigated agriculture. *J Hydrol* 329:281–293
- McDonald MG, Harbaugh AW (2003) The history of MODFLOW. *Ground Water* 41:280–283
- Neupane KM, Achet SH (2004) Use of backpropagation neural network for landslide monitoring: a case study in the higher Himalaya. *Eng Geol* 74:213–226
- Park E, Parker JC (2008) A simple model for water table fluctuations in response to precipitation. *J Hydrol* 356:344–349
- Pulido-Velazquez MA, Sahuquillo-Herraiz A, Ochoa-Rivera JC, Pulido-Velazquez D (2005) Modeling of stream–aquifer interaction: the embedded multireservoir model. *J Hydrol* 313:166–181
- Rasmussen WC, Andreasen GE (1959) Hydrologic budget of the beaverdam creek basin, Maryland. US Geological Survey Water-Supply Paper 1472, 106
- Ray RL, Jacobs JM (2007) Relationships among remotely sensed soil moisture, precipitation and landslide events. *Nat Hazards* 43:211–222
- Rushton KR, Redshaw SC (1979) Seepage and groundwater flow, 339. Wiley, Chichester
- Schmidt J, Dikau R (2004) Modeling historical climate variability and slope stability. *Geomorphology* 60:433–447
- Schwartz BF, Schreiber ME (2009) Quantifying potential recharge in mantled sinkholes using ERT. *Ground Water*. doi:[10.1111/j.1745-6584.2008.00505.x](https://doi.org/10.1111/j.1745-6584.2008.00505.x)
- Sophocleous M (1991) Combining the soil water balance and water level fluctuation method to estimate natural groundwater recharge: practical aspects. *J Hydrol* 124:229–241
- State of Florida department of transportation (2004) Stormwater management facility handbook. 69–70
- Szilagyi J, Harvey FE, Ayers JA (2005) Regional estimation of total recharge to ground water in Nebraska. *Ground Water* 43(1):63–69
- Trigo RM, Žezere JL, Rodrigues ML, Trigo IF (2005) The influence of the North Atlantic Oscillation on rainfall triggering of landslides near Lisbon. *Nat Hazards* 36:331–354
- U. S. Geological Survey (2009) <http://landslides.usgs.gov/monitoring/woodway/rtd/pressure.php>. Access 15 Jan 2009
- Van Asch ThWJ, Buma J, Van Beek LPH (1999) A view on some hydrological triggering systems in landslides. *Geomorphology* 30:25–32
- Wu J, Zhang R, Yang J (1996) Analysis of Precipitation-recharge relationships. *J Hydrol* 177:143–160